Common and Selective Molecular Determinants Involved in Metabotopic Glutamate Receptor Agonist Activity

Hugues-Olivier Bertrand,[†] Anne-Sophie Bessis,[‡] Jean-Philippe Pin,[§] and Francine C. Acher*[,‡]

Accelrys, Parc Club Orsay Université, 20 rue Jean Rostand, 91893 Orsay Cedex, France, Laboratoire de Chimie et Biochimie Pharmacologiques et Toxicologiques, UMR8601-CNRS, Université René Descartes-Paris V, 45 rue des Saints-Pères, 75270 Paris Cedex 06, France, and Centre INSERM-CNRS de Pharmacologie-Endocrinologie, UPR 9023-CNRS, 141 rue de la Cardonille, 34094 Montpellier Cedex 5, France

Received July 12, 2001

Several potent and group selective agonists of metabotropic glutamate receptors (mGluRs) have been docked at mGlu1,2,4R binding sites in the closed conformation of the bilobate extracellular domain. Quisqualic acid and (*S*)-3,5-dihydroxyphenylglycine (3,5-DHPG) were selected for mGlu1R, dicarboxycyclopropylglycine (DCG-IV), LY354740, (*S*)-4-carboxyphenylglycine (4CPG) for mGlu2R, and (*S*)-2-amino-4-phosphonobutyric acid (AP4), 1-aminocyclopentane-1,3,4-tricarboxylic acid (ACPT-I), (*S*)-4-phosphonophenylglycine (PPG) for mGlu4R. The models show a conserved binding pattern for the glycine moiety (α-amino and α-acidic functions) and group specific bindings for the distal acidic function. The best agonists allow optimized interaction with both lobes of the binding domain. Interlobe connections around the ligand are also described and participate in stabilizing the closed form of the amino-terminal domain. Altogether, the docking models support the proposal that the stabilization of a closed state represents a key step in agonist activation of mGluRs.

Introduction

Glutamic acid **1** (Chart 1) is the major excitatory neurotransmitter in the brain. Besides its physiological functions, it is involved in many neuropathologies. The excitotoxicity of glutamate is well established in ischemia, convulsions, and epilepsy. Glutamate is also implicated in neurodegenerative diseases such as Huntington's and Parkinson's diseases, in drug withdrawal symptoms, in pain and in psychiatric disorders such as anxiety and schizophrenia. Thus, glutamate receptors are excellent therapeutic targets.[1] There are two main types: the ion-gated-channel receptors, called ionotropic glutamate receptors (iGluRs), and the G-protein-coupled receptors, called metabotropic glutamate receptors (mGluRs).[2] While the iGluRs have been extensively studied for more than two decades, it is only rather recently that the mGluRs have been perceived as valuable therapeutic targets.[3,4] Yet, the elucidation of the physiological roles of each mGluRs and the discovery of new drugs depend on potent and selective ligands that are still lacking in many cases.[5−7] While antagonists can be found by high throughput screening, this technique might be less successful in the case of agonists or positive allosteric modulators. In fact, a detailed knowledge of the binding site and activation mechanism would allow the rational design of new ligands. The present study was undertaken for this purpose.

The mGluRs are divided into three groups according to their sequence similarity, transduction mechanism, and pharmacological profile.[2,8] Group I receptors (mGlu1,-5R) activate phospholipase C, while group II (mGlu2,-3R) and group III (mGlu4,6,7,8R) inhibit adenylyl cyclase when expressed in heterologous systems.[2] The most potent agonist of group I mGluRs is quisqualic acid **2**; it does not activate group II and III receptors but activates iGluRs of the AMPA type. Thus, (*S*)-3,5-DHPG **3** is preferred as a selective group I agonist, although it is less potent.[5,6] L-CCG-I **4** activates all mGluRs; however, its derivative, DCG-IV **5**, is a potent agonist of group II and a competitive antagonist at group I and III receptors.[9] Yet, the most potent group II selective agonists are LY354740 **6**[10] and its derivatives **8**−**11**.[11,12]

Chart 1

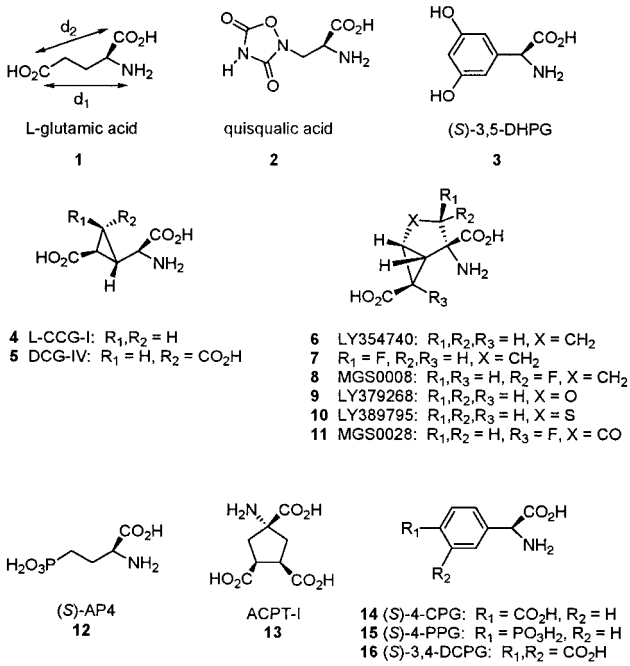

* To whom correspondence should be addressed. Phone: (33) 1 42 86 33 21. Fax: (33) 1 42 86 83 87. E-mail: acher@biomedicale.univ-paris5.fr.
† Accelrys.
‡ UMR8601-CNRS.
§ UPR 9023-CNRS.

10.1021/jm010323l CCC: $22.00
Published on Web 06/17/2002

(*S*)-AP4 **12** is recognized as the most potent group III agonist. It is also a weak antagonist of group II and has no effect at group I receptors.[5,6] ACPT-I **13**, although less potent, behaves similarly.[13,14] A particular mention should be made of phenylglycines bearing an acidic group in the 4-position of the aromatic ring. The (*S*)-4-carboxyphenylglycine 4CPG **14** is an agonist at mGlu2R, is an antagonist at mGlu1R, and has no effect at mGlu4R.[6] In contrast, (*S*)-4-phosphonophenylglycine PPG **15**[6,15] and (*S*)-3,4-dicarboxyphenylglycine (*S*)-3,4-DCPG **16**[16] are selective agonists of group III receptors. All of these phenylglycines (**14**−**16**) are characterized by longer distances between functional groups (d_1, d_2[17,18] > 6.5 Å, Chart 1) compared to the distances in glutamate and in the other analogues listed above.

Two conclusions were drawn from the study of pharmacophore models of mGlu1,2,4,8R agonists.[14,17,18] Glutamate activates all mGluRs in a similar extended conformation, and selectivity at the binding site would only result from the different protein environment. These conclusions were later confirmed by the three-dimensional model of the mGlu4R binding site[19] and the crystallographic structure of the mGlu1R ligand binding domain (LBD).[20] In this latter structure, extended glutamate (d_1 = 4.4 Å, d_2 = 5.0 Å) binds its three functional groups mainly as predicted by models.[19,21,22] Additionally, two water molecules seem to play a key role in tying the distal acidic group to the protein. While this paper was under revision, the structure of mGlu1R LBD bound with an antagonist (α-methyl-4-carboxyphenylglycine) was published.[23] Initially, a glutamate binding mode and insights into the activation mechanism were proposed by O'Hara when he discovered and validated some homology between the mGluR amino-terminal domain (ATD), to which glutamate would bind, and bacterial periplasmic binding proteins, such as LIVPB and LBP.[21] Thus, mGluR ATD was proposed to fold into two lobes connected by a hinge region, and the bilobate structure would close like a clamshell.[24] Indeed, both open and closed conformations proposed to be in dynamic equilibrium have been observed in different crystals.[20] The activation mechanism is initiated by the binding of glutamate or an agonist to one lobe of an open form, followed by the trapping of the ligand upon closure of the second lobe concomitant with an expulsion of water molecules. Furthermore, it has been demonstrated that mGluRs form homodimers linked at the level of the ATDs.[20,25] At least one closed-liganded conformation found in homodimers appears to be required to bring the dimer into an active state.[8,20,26] The agonist would stabilize the closed form, inducing a shift of the dynamic equilibrium to the active form.[27] In connection with this observation, we describe here, based on X-ray/homology models and ligand docking, how the most potent and selective agonists (Chart 1) could bind to their respective mGlu receptor types. Our data show that compared to glutamate, additional interactions between the ligands and the receptor allow a better stability of the closed-liganded form and are related to higher potency. In addition, these interactions are characteristic of the different receptor subtypes and are responsible for selectivity.

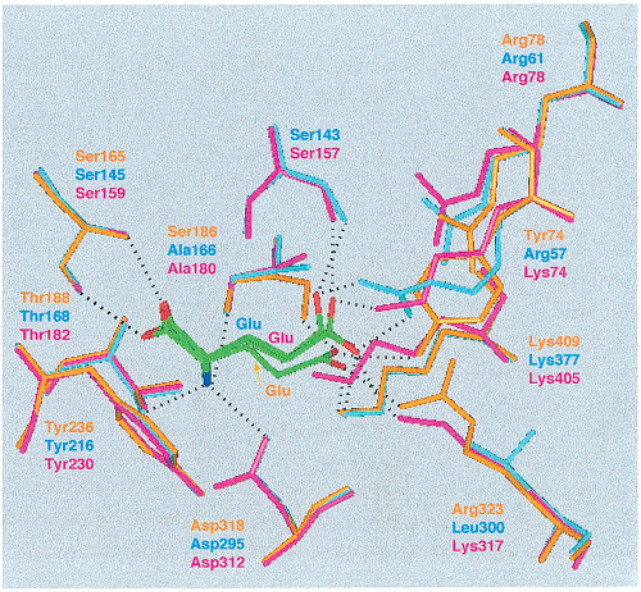

Figure 1. Superimposition of the three binding site models of mGlu1, mGlu2, and mGlu4 receptors docked with glutamate. The docking protocol was applied to glutamate in its pharmacophore conformation[17] and manually positioned in 1ewk:A without water molecules to generate the mGlu1R model (orange). The mGlu2 (cyan) and mGlu4 (magenta) receptor models were obtained similarly using the LBD models generated by MODELER. Glutamate carbon atoms are colored in green, nitrogen atoms in blue, and oxygen atoms in red. Its distal acidic function is roughly in the plane of the figure for mGlu2/4 receptors and perpendicular for the mGlu1 receptor.

Results

The coordinates of the closed and open forms of mGlu1R LBD bound with glutamate were retrieved from the Protein Data Bank (entries 1ewk:A and 1ewk:B, respectively). Models of the closed form of mGlu2,4R LBD bound with glutamate were generated by comparative modeling using 1ewk:A with glutamate as a template (see Materials and Methods, Figure 1). For each receptor, the most potent and selective agonists (Table 1) were taken in their bioactive conformation as determined by the pharmacophore models: quisqualic acid **2** and (*S*)-3,5-DHPG **3** for mGlu1R;[17] DCG-IV **5**, LY354740 **6**, its derivatives **7**−**11**, and (*S*)-4CPG **14** for mGlu2R;[17] and (*S*)-AP4 **12**, ACPT-I **13**, (*S*)-PPG **16**, and (*S*)-DCPG **17** for mGlu4R.[18] They were positioned into the receptors by superimposing their glycine entity onto that of glutamic acid in each model. They were docked according to a molecular mechanics/dynamics protocol allowing side chain and ligand flexibility. The general protocol includes a harmonic constraint on the Cα trace which is kept during the process. To evaluate the influence of the harmonic constraint, it was released in one model of each mGluR subtype. Since no changes were observed, the initial shorter protocol was adopted (see Materials and Methods). Although several water molecules bind to glutamate in the template 1ewk:A, none were put in our simulations, because their occurrence and position likely depend on the ligand and receptor subtype. To validate our docking protocol (without water molecules), it was applied to glutamate taken in its mGlu1R pharmacophore g^-a conformation[17] and docked in 1ewk:A. The resulting model was compared to the crystallographic structure. A similar

Table 1. Potencies, Binding Affinities, and Scoring Function Values of the Agonists Docked in the mGluR Binding Site Models

	mGlu1R					mGlu2R					mGlu4R				
ligands[a]	EC_{50}/IC_{50}[b] (μM)	K_i (μM)	Ligscore[c]	PLP1[c]	PMF PMF_H[c]	EC_{50}/IC_{50}[b] (μM)	K_i (μM)	Ligscore[c]	PLP1[c]	PMF PMF_H[c]	EC_{50}/IC_{50}[b] (μM)	K_i (μM)	Ligscore[c]	PLP1[c]	PMF PMF_H[c]
L-Glu **1**	1	0.34	6.1	85.2	50.2 154.6	5.9	1.2	5.8	76.8	35.6 129.8	20	1.6	6.2	74.4	37 141.7
(*S*)-3,5-DHPG **3**	3.4	0.9	6.5	94.4	63.3 176.6	ne[d]	$>10^3$				ne[d]				
Quis **2**	0.045	0.01	6.7	104.8	80.8 184.9	108	113				593	112			
4CPG **14**	*18*	3.7				692		6.1	87.4	38.2 138.4	$>10^3$	838			
DCG-IV **5**	*389*	77				0.35	0.11	6.0	87.3	52.6 140.9	*22.5*				
LY354740 **6**	*458*					0.02	0.013	6.5	93.3	47.3 182.3	*1009*				
(*S*)-AP4 **12**	ne[d]	$>10^3$				*295*	129				0.58	0.47	4.7	83.2	46.8 121.1
ACPT-I **13**	ne[d]					ne[d]					7.2		5.8	98.8	50.3 168.8
(*S*)-PPG **15**	ne[d]					ne[d]					5.2		4.2	104.3	46.7 142.1

[a] Binding references.[28−30,32,33,62] [b] IC_{50} values for antagonists are italic. [c] Scoring function references;[44−46] PMF and PMF_H refer to the PMF function without and with hydrogens, respectively.[46] [d] ne = no effect at 1 mM.

glutamate *aa* conformation, a similar position relative to the protein backbone, and similar polar bindings were detected (Figure 1). Distances between oxygen atoms of the γ-carboxylate and nitrogen atoms of Arg78 and Gly293 remained unchanged, leaving an empty space in place of the water molecules present in the crystal structure. In fact, because Arg78 is already stretched out in the presence of the water molecule, its side chain cannot further extend during MD without water. Indeed, similar weak ionic interactions are maintained and keep Arg78 well oriented. Hence, we have run all experiments without water. When the resulting models were analyzed, bridging water molecules could be suggested in some cases. They were then manually positioned, and the resulting system was submitted to final minimization.

Agonist bindings were analyzed in their respective models (Figures 1−4). A qualitative correlation with binding affinities[28−34] is outlined; however, no precise quantification was performed. Several approaches have been proposed to correlate receptor−ligand interactions (hydrogen bonding, Coulombic interactions, hydrophobic interactions, entropy, and solvation) with binding affinities or efficacies.[35,36] However, our simulations do not allow an accurate determination of binding energies. Nevertheless, a rank-ordering based on scoring functions for docked poses is proposed.

mGlu1R. The proximal amino and acidic functions of glutamate **1**, quisqualic acid **2**, and (*S*)-3,5-DHPG **3** bind similarly to the receptor. Binding to the first lobe (I) is established through a network of hydrogen bonds between the carboxylate, the amino group, and Ser165, Thr188, and Ser186 (backbone carbonyl) (Figures 1 and 2). Binding to the second lobe (II) is secured by an ionic interaction between the ammonium and Asp318 side chain function and by a cation−Π interaction[37] between this protonated group and the aromatic moiety of Tyr236[19,20] (Figures 1 and 2). This positively charged group can also interact with the negative charge of Asp208 which is more distant and located in the hinge region. Moreover, the α-proton of all ligands points to the aromatic cycle of Tyr236, making a stabilizing CH−Π interaction.[38] With **1**−**3**, we note that the distal acidic function is bound to Tyr74, Arg323, and Lys409. However, a weaker cation−Π interaction between the aromatic ring of **3** and the ammonium of Lys409 is found in place of the ionic interaction between **1** or **2** and Lys409. In 1ewk:A, three other residues, Arg78, Ser186, and Gly293, bind to the γ-carboxylate of glutamate via two water molecules which seem to play an important role in anchoring the ligand into the cleft.[20] Interestingly, in our models, direct binding is observed between these residues and **2** or **3**. Indeed, with (*S*)-3,5-DHPG **3** the 3-phenol function is bound directly to Ser186, and the 5-phenol is linked to Gly293. Similarly, the dioxo groups of quisqualate bind directly to these residues. Additional contacts between Trp110, Gly319, and ligands stabilize the complex. While glutamate 3-pro*S* and 4-pro*S* protons are in van der Waals contact with Trp110 H7 and a Gly319 proton, respectively, CH−Π interactions and van der Waals contacts are detected between H6 and H7 of Trp110, a Gly319 proton, and the aromatic ring of **3** (Figure 2A). With quisqualic acid, it is noteworthy that all bindings are very well fitted,

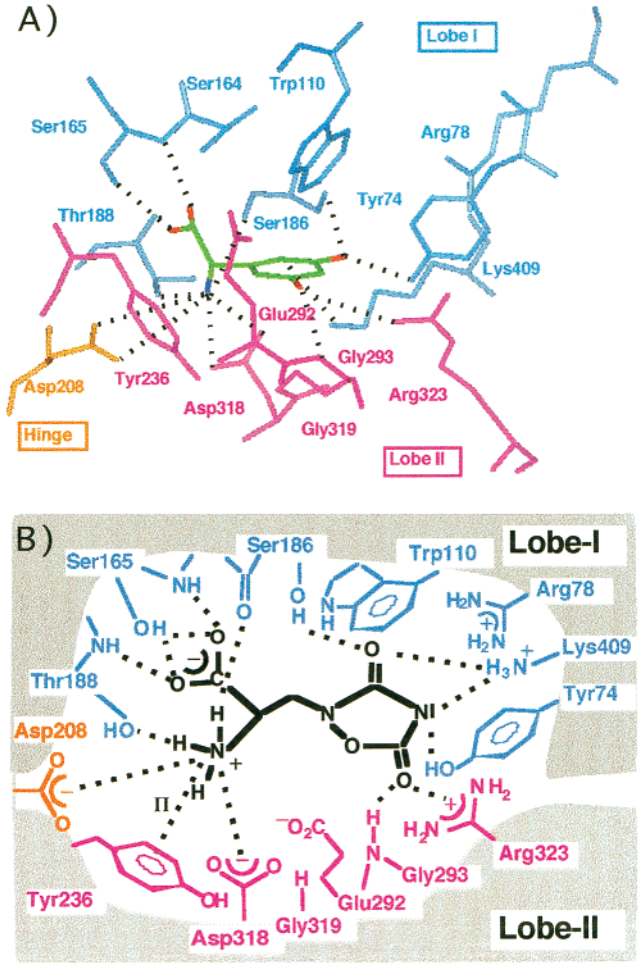

Figure 2. (*S*)-3,5-DHPG **2** (A) and quisqualic acid **3** (B) docked at the mGlu1R binding site. A scheme is shown for quisqualate. Residues of lobe I are colored in blue, those of lobe II in magenta, and Asp from the hinge is in yellow. In panel A, ligand carbon atoms are in green, oxygens in red, and nitrogens in dark blue; hydrogen atoms have been omitted for clarity. In panel B, ligand atoms are black. Polar interactions between ligand and protein are represented by black dotted lines.

and the heterocycle binds optimally to Tyr74, Ser186, Gly293, Arg323, and Lys409 (Figure 2B). Furthermore, all atoms of the heterocycle besides N4 are in van der Waals contact with H6 or H7 from Trp110. Thus, it seems that binding to both lobes is optimized with quisqualic acid so that the closed conformation of the LBD is best stabilized. It should also be mentioned that several couples of residues from the two lobes interact to secure the closing of the bilobate structure as Ser166−Asn235 and Trp110−Glu292 which are close to the ligand, and these are maintained with all agonists (see below).

mGlu2R. The proximal amino and acidic functions of glutamate **1**, DCG-IV **5**, LY354740 **6**, its derivatives **8**−**11**, and (*S*)-4CPG **14** are all bound similarly to the receptor by residues which are homologous to those of mGlu1R: Ser145, Thr168, and Ala166 (backbone carbonyl) from lobe I; Asp295 and Tyr216 from lobe II; and Asp188 from the hinge region (Figures 1 and 3). The same set of connections, as with mGlu1R, is established. The distal acidic function is bound to lobe I by means of hydrogen bonds and ionic interactions with Arg57, Arg61, and Lys377 (Figure 3). No direct polar anchoring

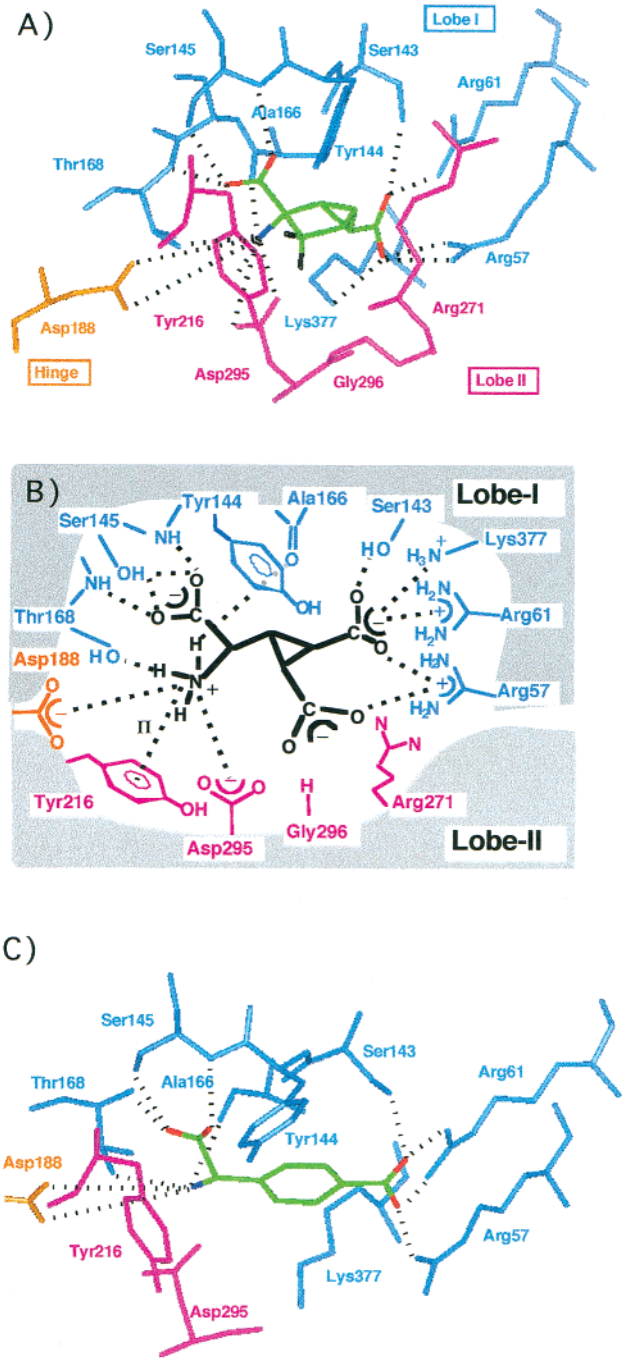

Figure 3. LY354740 **6** (A), DCG-IV **5** (B), and (*S*)-4CPG **14** (C) docked at the mGlu2R binding site. A scheme is shown for DCG-IV **5**. Residues and ligand atoms are colored as in Figure 2. Hydrogen atoms (black) have been omitted for clarity except for the C3 protons of **6** which are discussed in the text. Polar interactions between ligand and protein are represented by black dotted lines.

to lobe II is observed in this region, although water molecules may still bridge the γ-acidic group to the lobe II backbone as observed at the mGlu1R binding site with Gly293. However, several links between the two lobes provide a tight closing in this region. In particular, the Arg271 (lobe II) guanidinium group makes a hydrogen bond with Ser93 (lobe I) and a cation−Π interaction with Tyr144 (lobe I) which, in turn, is connected to lobe II via the backbone carbonyl of Glu213. Interestingly, the two residues Ser93−Arg271 are homologous to Trp110−Glu292 from mGlu1R. Moreover, for the

most potent agonist LY354740 **6**, van der Waals contacts are detected between the methylene protons of the Arg271 side chain and its C4 hydrogens. Thus, an additional link to lobe II is established (Figure 3A). The docking of DCG-IV **5** reveals that its additional acidic group is mainly bound to Arg57 from lobe I. Therefore, it would not provide an additional strong interaction with lobe II (Figure 3B), affording a possible explanation for its potency being equal to that of L-CCG-I **4**. In addition, the increased activity of **6** compared to that of **4** and **5** suggests that entropic gain induced by constrained extended conformations is also responsible for the enhanced activity.[39,40] As noted for mGlu1R, the α-proton of glutamate and analogues, such as L-CCG-I **4** or DCG-IV **5,** points to the aromatic ring of Tyr216 making a CH−Π interaction. In **6**, this contact occurs with the 3-pro*R* proton. Thus, when this proton is replaced by a fluorine atom, as in **7**, a repulsive interaction between the negative density of the aromatic ring and the fluorine likely destabilizes the closed form of the ATD.[41] Hence, **7** would not activate the receptor and turned out to be an antagonist.[12] This repulsion does not take place when the 3-pro*S* proton of **6** is substituted by a fluorine atom, as in **8**, because it is oriented differently, and it does not affect the closing of lobe II. Similarly, when the α-proton of L-CCG-I **4** is replaced by a methyl group, optimal closing of lobe II is also prevented, and the resulting compound (MCCG-I) is turned into a competitive antagonist. This observation will be reported in due course. The analysis of the mGlu2R models docked with several agonists (**1**, **4**−**6**, **9**−**11**) suggests that a water molecule might be situated between Arg61 and the agonist distal acidic group. It would also be bound to Ser143. It was manually positioned in the docking model of **6** as an example, and the resulting system was minimized (Figure 5A). With **9**−**11**, a second water molecule is probably bridging the intracyclic heteroatom (O or S) or the 4-carbonyl group[42] to Ser272 and Glu273 (lobe II), thus, reinforcing the connection between the ligand and lobe II, as shown for **11** in Figure 6. Furthermore, a new hydrogen bond is disclosed between the 6-fluorine of **11** and the ammonium group of Lys377 (Figure 6). (*S*)-4CPG **14** binds like the shorter agonists mentioned above, except for Lys377 whose amino group is turned away from the ligand, keeping a strong interaction with Glu318 from the hinge region and Asp295 (Figure 3C). In the present model, the 4-carboxyphenyl moiety is tucked into lobe I and interacts tightly with Arg57 and Arg61. In this case, no water molecule would be bridging the ligand to Arg61.

mGlu4R. The proximal functions of glutamate **1**, (*S*)-AP4 **12**, ACPT-I **13**, (*S*)-PPG **15**, and (*S*)-DCPG **16** are tied up to the conserved residues Ser159, Ala180 (backbone carbonyl), Thr182, Asp202, Tyr230, and Asp312 by the same binding network as mGlu1R and mGlu2R, as described previously[19,43] (Figures 1 and 4). The distal acidic functions are surrounded by an impressive number of basic and hydrophilic residues: Lys74, Arg78, Ser157, and Lys405 from lobe I and Arg258, Asn286, Ser313, and Lys317 from lobe II (Figure 4). We noticed that the two oxygen atoms of the γ-carboxylate in **1** are directly linked to residues from lobe I and to Lys317 from lobe II (Figure 1), while other

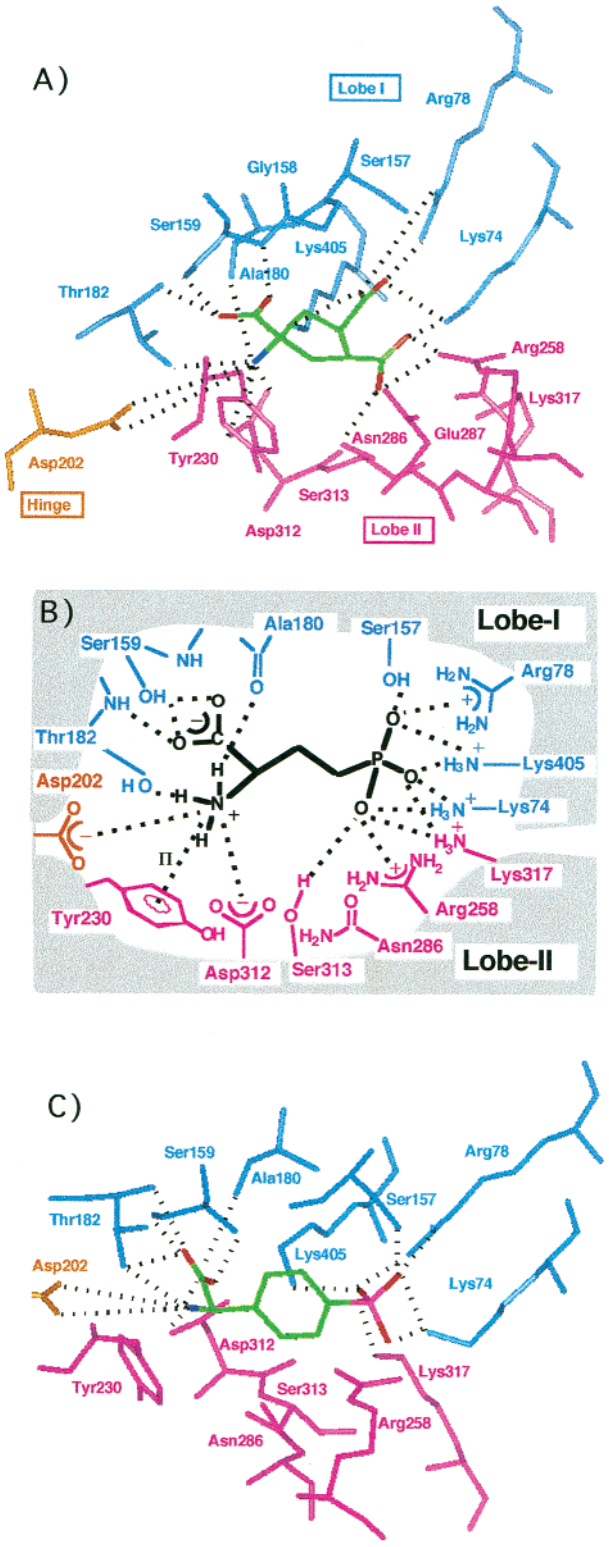

Figure 4. ACPT-I **13** (A), (*S*)-AP4 **12** (B), and (*S*)-PPG **15** (C) docked at the mGlu4R binding site. A scheme is shown for (*S*)-AP4 **12**. Residues and ligand atoms are colored as in Figure 2, and phosphorus atom are in magenta. Hydrogen atoms have been omitted for clarity. Polar interactions between ligand and protein are represented by black dotted lines.

connections to lobe II residues are probably established by means of water molecules which are not present in our models. Yet, with ACPT-I and (*S*)-AP4 direct binding takes place. Binding to Lys74, Ser157, and Lys405 from lobe I is observed, while Arg78 makes a weak ionic interaction or binds via a water molecule to the ligand

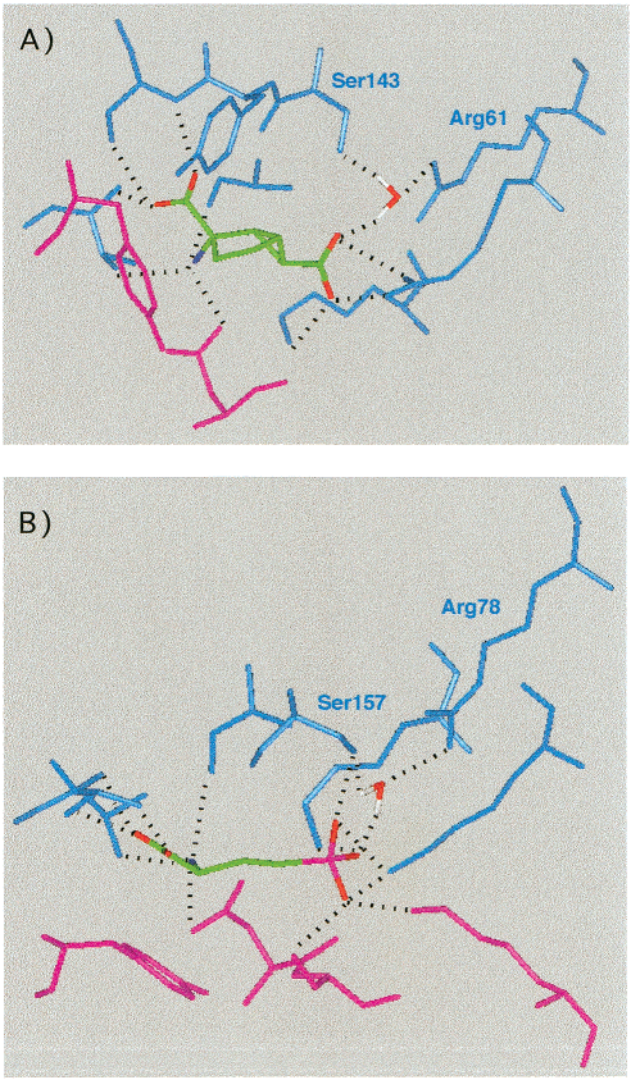

Figure 5. Putative water molecule bridging the agonist distal acidic function and the conserved arginine in the models of mGlu2 (Arg61) and mGlu4 (Arg78) receptor LBD. The water molecule was manually positioned in the **6**/mGlu2 (A) and **12**/mGlu4 (B) receptor models, and the resulting systems were minimized.

distal carboxylate or phosphonate (see below). Arg258, Asn286, Ser313, and Lys317 from lobe II are bound to the distal functions of ACPT-I (Figure 4A). Similar residues interact with the phosphonate group of (*S*)-AP4; however, because of its smaller size compared to the combination of two carboxylates, Arg258 and Asn286 stand aside from the ligand, decreasing the interactions of the phosphonate with these residues (Figure 4B). The two phenylglycines, (*S*)-PPG **15** and (*S*)-DCPG **16**, fit nicely to the cluster of basic residues. The (*S*)-PPG phosphonate group is more distant from the glycine moiety than it is within (*S*)-AP4; thus, some of the (*S*)-AP4 bindings are absent (Ser313), weaker (Arg258), similar (Lys74, Ser157, Lys317, and Lys405), or stronger (Arg78) (Figure 4C). (*S*)-DCPG **16** binds to similar residues (data not shown). Both phenylglycines bind directly to Arg78 with no bridging water molecule as observed for (*S*)-4-CPG **14** at the mGlu2R binding site. On the other hand, shorter agonists, such as **12** and **13**, may be linked to Arg78 by means of a water molecule. Such a water molecule was manually positioned in the docking model of **12** as an example, and the resulting

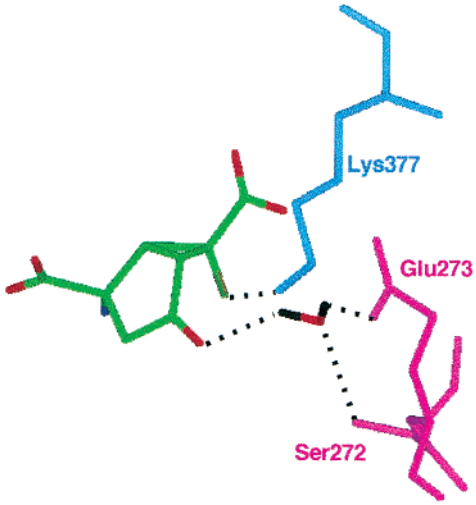

Figure 6. Proposed water molecule bridging the carbonyl group of **11** and selected residues of lobe II (magenta). The hydrogen bond between the 6-fluoro substituent (dark green) and Lys377 of lobe I (blue) is displayed. Atoms of **6** and of the water molecule are colored as in Figure 2. Polar links are indicated as dotted lines. The water molecule was manually positioned in the final minimized **11**/mGlu2R LBD complex, and the system was submitted to the minimization protocol.

system was minimized (Figure 5B). We notice that Ser157 is also bound to the bridging water.

Model Scoring. To correlate agonist affinities and suggested binding modes, we have scored our models using several scoring functions (Ligscore,[44] PLP1,[45] and PMF with or without consideration of hydrogen atoms[46]) as implemented in the Cerius2−LigandFit module.[44] Scoring functions are mostly used to discriminate between active and inactive compounds in the process of virtual screening.[47] However, a correlation between binding affinities and the predicted scores of the docked compounds has been achieved in some cases.[48,49] Scores of the docking models presented above are displayed in Table 1. With the three functions, the same rank order is observed for mGlu1 agonists: Glu < (*S*)-3,5-DHPG < Quis. Glutamate and (*S*)-3,5-DHPG show affinities and potencies in the same range and close scoring values. Quisqualate is more potent; this is best revealed using PMF.[46] With mGlu2R, the binding affinity trend is recovered using Ligscore, PLP1, and PMF_H: Glu < DCG-IV < LY354740. With mGlu4R, PLP1 and PMF values are the lowest for glutamate (Table 1) and similar for the three agonists (*S*)-AP4, ACPT-I, and (*S*)-PPG. Glutamate's affinity is indeed weaker than that of (*S*)-AP4. Binding affinities are not available for ACPT-I and (*S*)-PPG, yet their binding mode is analogous to that of (*S*)-AP4 as expressed by the scoring values.

Agonist Selectivity. When the Cα traces of mGlu2 and mGlu4 receptor models docked with glutamate are superimposed onto the traces of 1ewk:A, we notice that the glycine moieties of all ligands coincide perfectly. Nevertheless, a slight shift of the distal function is observed in the type 2 and 4 models (Figure 1). As a result, the γ-acidic function is more buried in lobe I in the models of mGlu2/4R, and more space is available between the glutamate tied to lobe I and the residues of lobe II. Hence, larger agonists are well accepted at the mGlu2/4R binding site (see below). Moreover, the orientation of the distal carboxylate is quite different

between the type 1 model and the type 2 and 4 models. In the case of the mGlu1 receptor, the γ-carboxylate lies roughly in a plane that contains the α-proton, while in the two other cases, the plane is roughly perpendicular to this proton (Figure 1).

With competitive antagonists, we assume that in most cases binding to lobe I takes place, but the adjusted closing is disrupted as described with AMPA receptors.[50] Several group II agonists (DCG-IV, LY354740, and (*S*)-4CPG) are group I antagonists (Table 1). They bind to the active site of the ATD, as indicated by binding affinity values (Table 1), but optimal closing may not be reached. Therefore, docking of competitive antagonists in open forms may be considered but not in closed ones. DCG-IV **5** can bind to the ATD first lobe; however, upon closing, the additional carboxylic group probably makes a repulsive interaction with Glu292 and interferes with the Glu292−Trp110 interlobe connection (see below). With LY354740 **6**, the rigid bicyclic structure cannot fit in the space delimited by the side chain of Tyr236 upon the closing of the group I ATD (Figure 7A). With (*S*)-4CPG **14**, the longer distances between functional groups (d_1 = 6.5 Å, d_2 = 6.8 Å) induce a displacement of Tyr74 in the model of the ATD open form (Figure 7B). Tyr74 plays a critical role in positioning the distal function of ligands and in the arrangement of residues around this function: Trp110 CH−Π interactions and Arg71, Arg78, and Arg323 cation−Π interactions. The displacement of Tyr74 in the open-liganded form of ATD also prevents the formation of the Tyr74−Arg323 interlobe connection during closing and would be responsible for antagonist property (Figure 7B). Also, in the minimized open system, the amino group of the phenylglycine is not pointing to Tyr236 as expected for regular closing. In group II and III receptors, Tyr74 (mGlu1R) is replaced by residues which allow more flexibility to bind longer agonists (Arg57 in mGlu2R and Lys74 in mGlu4R).

In contrast to group II agonists, group III agonists, (*S*)-AP4, ACPT-I, and (*S*)-PPG, do not display any activity at mGlu1/5R or at mGlu2/3R. (*S*)-AP4 **12** is structurally very close to glutamate **1** and, nonetheless, does not show any activity or affinity for mGlu1R (Table 1). Because of this lack of affinity, we suggest that (*S*)-AP4 cannot bind its functional groups to the open form of the ATD. This step would be required before the closing motion. Thus, we have positioned (*S*)-AP4 in place of glutamate in 1ewk:B (open form template) and minimized the system with a constraint on the Cα trace and ligand d_1 distance because of a propensity to adopt a folded conformation due to internal ionic interaction. The resulting model is shown in Figure 7C and is compared to 1ewk:B. Tyr74 is displaced as with (*S*)-4CPG. Additionally, a disrupted hydrophobic network might be responsible for the inability of (*S*)-AP4 to bind to the protein. In fact, a hydrophobic pocket located in lobe I close to the hinge seems to play a critical role in the stability of the mGlu1R bilobate structure. It is composed of Thr188 (methyl group), Val205, Pro206, Phe412, and Lys409 (methylene groups) of lobe I and Leu342 from the hinge region. In particular, the Lys409 δ and ϵ methylene groups are in van der Waals contact with a Leu342 methyl group. Moreover, the Lys409

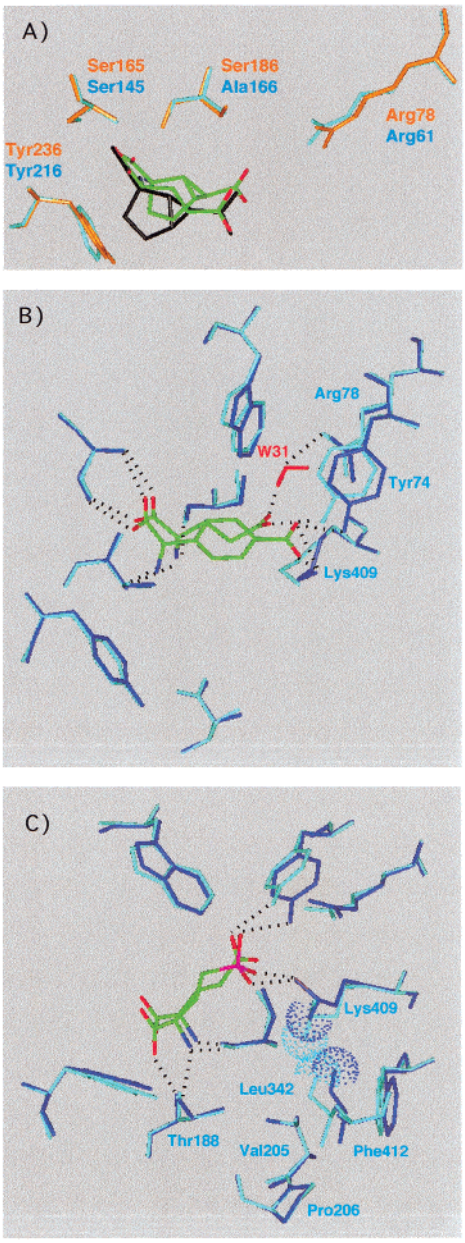

Figure 7. (A) Superimposition of mGlu1R and mGlu2R binding sites, as described in Figure 1, with bound glutamate (mGlu1R) and LY354740 (mGlu2R). The color code is the same as in Figure 1. In addition, the amino and acidic functions of LY354740 (black) have been superimposed over those of glutamate in mGlu1R. This disposition shows that the additional rigid cycle of LY354740 would be in a steric clash with Tyr236, because its γ-carboxylate is not as deeply buried in lobe I as in the mGlu2R model. (B and C) Proposed anchoring of (*S*)-4-CPG **14** (B) and (*S*)-AP4 **12** (C) in the open form of mGlu1R LBD (1ewk:B). Ligands were manually positioned in the crystal structure, and the resulting system was submitted to the minimization protocol. These models (dark blue) were then superimposed (Cα trace) onto the 1ewk:B structure (cyan) with bound glutamate. Water molecule W31 from lewk:B is displayed in panel B. Compounds **14** and **12** exhibit similar bindings as glutamate; however, critical residue side chains have shifted as with Tyr74, Lys409, and Leu342. Ligand carbon atoms are colored in green, oxygens in red, nitrogens in dark blue, and phosphorus in magenta. Hydrogen atoms have been omitted for clarity except for two specific ones from Lys409 and Leu342 which are in contact in the initial structure and apart after minimization (panel B). They are displayed as van der Waals spheres.

amino group interacts with the distal acidic function of the ligands. Thus, a change in this ionic interaction may induce a loss of the critical van der Waals contact as illustrated with the binding of (*S*)-AP4 to the open form of ATD (Figure 7C). The same hydrophobic contacts are found in the type 2 receptor (Thr168, Val185, Pro186, Phe380, Lys377, and Leu319). However, Leu342 (mGlu1R) aligns with Pro336 in mGlu4 such that hydrophobic interactions would not be disrupted by the binding of (*S*)-AP4 in the latter receptor. The selectivity of (*S*)-AP4 might also be related to the position of specific water molecules on which we have currently no data.

Interlobe Connections. In addition to the binding of the agonist to the second lobe when the ATD closes, several interlobe connections occur (Figure 9). These are localized all along the cleft defined by the two lobes. In the present article, we focus on those situated near the ligand and which could affect ligand binding. In any case, these interactions occur regardless of which agonist is docked in the binding site. Thus, they are shown for mGlu1R with (*S*)-3,5-DHPG, mGlu2R with DCG-IV, and mGlu4R with ACPT-I docked at the binding site (Figure 8). The interlobe connections can be divided, for each receptor, into three sets of residues linked by polar interactions (Figures 8 and 9). The first set is composed of 5 conserved residues (Figure 9A). All of these, besides Gln, also interact with the ligand. Asp from the hinge is part of this set, because it participates in positioning residues from lobe I (Thr) and lobe II (Gln). This Gln residue is bound to a second Asp which makes the second interlobe connection of the set with Lys (Figures 8 and 9A). The second set holds mostly conserved residues; however, some connections are particular to one type of receptor (Figure 9B). The link found in mGlu1R between Ser166 and Asn235 is also detected between the homologous residues of mGlu2R (Asp146 and Asn215) and mGlu4R (Ser159 and Ser229). The second interlobe connection of this set is found between Ser189 and Asn235 of mGlu1R and between Ser169 and Asn215 of mGlu2R (Figures 8 and 9B) but not between homologous residues in mGlu4R (Ala183 and Ser229). On the other hand, Ser229 is bound to Ser233 (part of the same g−F loop[20]) which, in turn, is bound to Asp185 close to Ala183. In the third set, residues located around the distal function of the ligand are involved. Connections are mostly specific to each receptor, although residues involved are found in a limited number of loops (Figures 8 and 9C). Among the four interlobe connections detected in mGlu1R, two of them, Arg71−Glu325 and Tyr74−Arg323, are specific and are found in neither mGlu2R nor mGlu4R. The two others, Trp110−Glu292 and Ser164−Glu292, are also present in mGlu2R with Ser93−Arg271 and Tyr144−Arg271. In these two cases, Glu292 (mGlu1R) and Arg271 (mGlu2R) from lobe II line the ligand and anchor to the two residues of lobe I as pliers. In mGlu2R, the cation−Π interaction between Arg271 and Tyr144 is also reinforced by a hydrogen bond between Tyr144 and Glu213 which is lacking in mGlu1R. For subtype 4, Asn286, the homologue of Glu292 in mGlu1R and Arg271 in mGlu2R, is only bound to the ligand and does not participate in interlobe interaction. Yet, its neighboring residue Glu287 is linked to Lys74 of lobe I (Figures 8 and 9C). Another

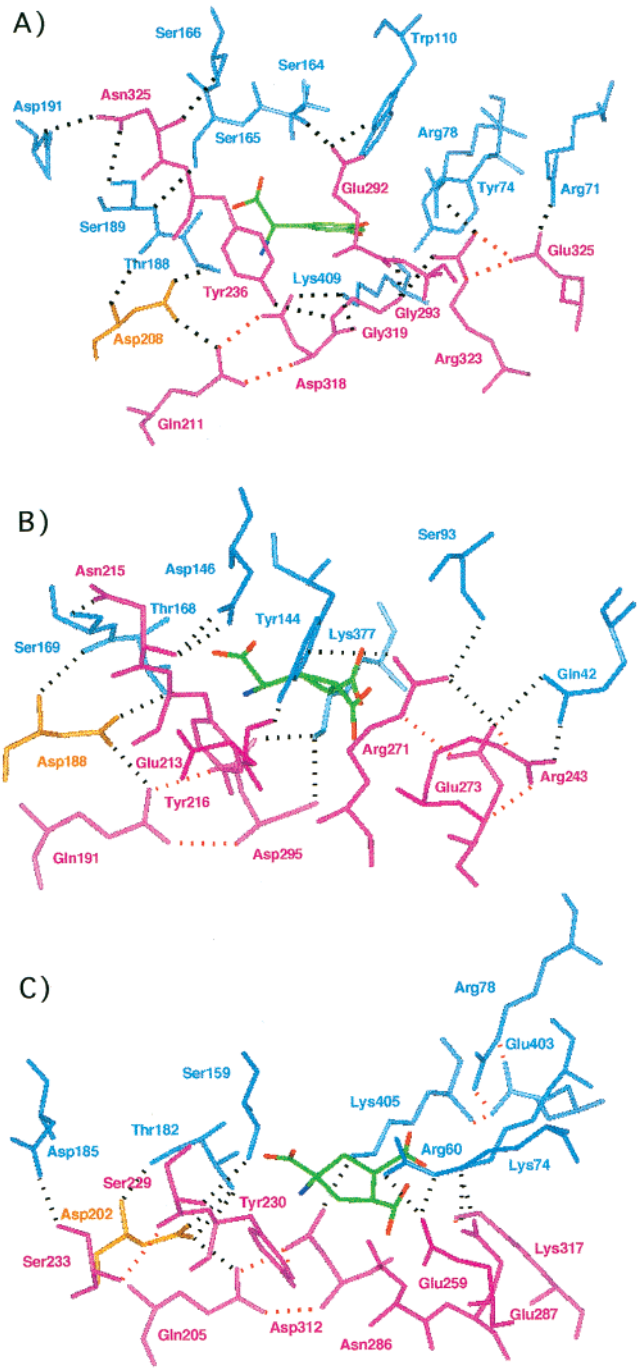

Figure 8. Networks of polar interactions (dotted lines) between the two lobes of mGlu1R docked with **3** (A), mGlu2R docked with **5** (B), and mGlu4R docked with **13** (C). Atoms and residues are colored as in Figure 2 with interlobe connections in black and intralobe connections in red.

pliers-type connection is also observed in mGlu2R with Gln42 (loop b−A) linking Arg243 (loop h−G) and Glu273 (loop i−H). In mGlu4R, a partly similar connection occurs with Arg60 (loop b−A) interacting with Glu259 (loop h−G) and Ser110 from lobe I that is homologous to Trp110 (mGlu1R) and Ser93 (mGlu2R) (Figures 8 and 9C).

Discussion

A Common Motif Binds the Glycine Moiety. Although flexibility of both side chains and ligand was allowed in all runs, the initial binding pattern of the

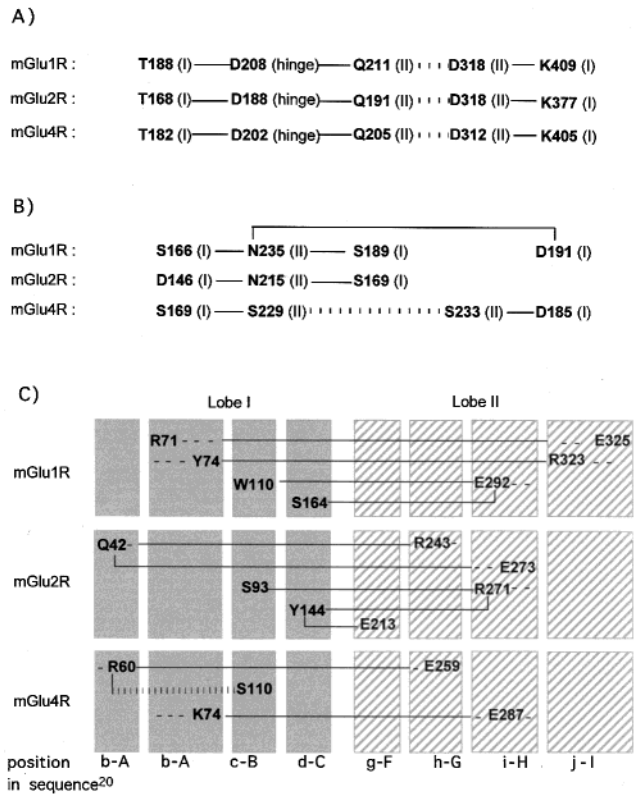

Figure 9. Schematic representation of the 3 sets of interlobe connections close to the ligand. Panels A and B: proximal and mostly conserved interactions. Lobe I, II, or hinge is indicated in brackets. Panel C: specific interactions around the distal function of the agonist. The residues involved in these connections belong to three loops from lobe I and four loops from lobe II which are boxed in dark and hatched gray, respectively. In all cases, they are situated between a β-sheet and an α-helix which are named according to Kunishima.[20] Interlobe interactions are shown with solid lines, and intralobe ones are shown with dashed lines.

Table 2. Conserved Residues of Rat mGluRs, DmGluAR, Rat CaSR, LIVBP/LBP, and Goldfish OR5.24 Binding to the Glycine Moiety of Agonists[a]

mGlu1R	S165	S186[b]	T188	D208	Y236	D318
mGlu5R	S151	S172[b]	T174	D194	Y222	D304
mGlu2R	S145	A166[b]	T168	D188	Y216	D295
mGlu3R	S151	A172[b]	T174	D194	Y222	D301
mGlu4R	S159	A180[b]	T182	D202	Y230	D312
mGlu6R	S148	A169[b]	T171	D191	Y219	D301
mGlu7R	S159	A180[b]	T182	D202	Y230	D314
mGlu8R	S156	A177[b]	T179	D199	Y227	D309
DmGluAR	S158	A179[b]	T181	D201	Y229	D310
CaSR	S147	A168[b]	S170	D190	Y218	E297
LIVBP	S79	A100[b]	T102	D121	Y150	E226
LBP	S79	G100[b]	T102	D121	Y150	E226
OR5.24	S152	A173[b]	T175	D195	Y223	D309

[a] Figure 10. [b] Residue bound to the ligand through its backbone oxygen atom.

glycine moiety was maintained. Indeed, our modeling approach revealed that all agonists docked at their respective mGluR binding site display a similar mode of binding for their glycine entity. The α-carboxylate and α-ammonium groups are bound to lobe I of the receptor by way of an analogous hydrogen bond network that implies a conserved Ser and Thr and a homologous backbone carbonyl group (Table 2 and Figure 10). Such interactions have been clearly identified in the crystal structures of LIVBP and mGlu1R ATD, solved with their bound ligand, leucine[51] and glutamate,[20] respectively. Only the amino function is directly anchored to lobe II through an ionic and a cation−Π interaction with a conserved Asp and Tyr, respectively, and anchored to the hinge region by an electrostatic interaction with a conserved Asp (Table 2 and Figure 10). The five residues that anchor the glycine moiety are conserved in the same structural family members that are known to bind amino acids, such as leucine isoleucine valine binding protein (LIVBP), leucine binding protein (LBP),[51,52] DmGluAR,[53] calcium-sensing receptor (CaSR),[54] and odorant receptors OR5.24,[55] and may, therefore, constitute a motif for amino acid binding in this family of proteins containing an LIVBP-like domain. Indeed, these proteins were retrieved when a sequence search was run with the mGlu1R ATD sequence and the aforementioned pattern. These results will be reported elsewhere.

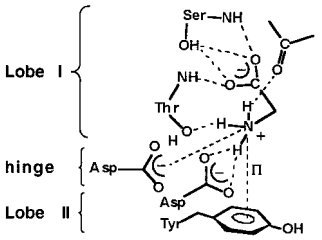

Figure 10. Synthetic scheme of the conserved binding residues of the glycine moiety (Table 2).

Binding Site Water Molecules. The X-ray structure[20] reveals that two water molecules named 46H and 11H in 1ewk:A provide links between the glutamate distal function and receptor lobes I and II, respectively. The water molecule 46H is also present in the crystal structure of the open-liganded form monomer 1ewk:B.[20] This suggests that it might be part of the structure of the glutamate binding site. Moreover, this water molecule is bound to Arg78 which is conserved among all mGluRs and may be part of all subtype binding sites. However, this water molecule is also bound to Ser186 which is conserved in group I receptors only and aligns with an alanine in other receptors (Table 2). Other serine residues conserved in groups II and III are present in the vicinity of the conserved arginine (Ser93/110, Ser143/157, and Ser167/181 in mGlu2/4R, Table 3) and could play the previous serine's part. Yet, docking experiments were run without water for the following reasons. We have a priori no indications of how a water molecule would be positioned. Indeed, it has been shown that the conservation or displacement of active-site-bound water is highly influenced by the protein microenvironment of the water molecule.[56] It was also noted that the average improvement of the predicted water molecule was minor in a series of 200 protein−ligand complexes.[57] Moreover, with bulkier agonists, water molecules may be displaced or ejected from the site.[58] These comments also apply to water molecule 11H bridging glutamate to the amide proton of Gly293 in mGlu1R. Interestingly, we checked with the glutamate/mGlu1R model that the side chains of binding site residues are well positioned in our conditions (Figure 1). In return, binding site water molecules could be proposed for the **6**/mGlu2R and **12**/mGlu4R models.

Selectivity Is Located around the Distal Function. Despite two conserved basic residues (Arg and Lys,

Table 3. Residues that Interact with the Distal Function of Glutamate and Agonists, in the Closed Conformation of the ATD of Rat mGluRs

	lobe I								lobe II				
mGlu1R	**Y74**[a]	***R78***	**W110**	**G163**	**S164**	**S186**	**A187**	***K409***	S263	**E292**	**G293**	**G319**	**R323**
mGlu5R	Y64	*R68*	W100	G149	S150	S172	A173	*K395*	S249	E278	G279	G305	R309
mGlu2R	**R57**	***R61***	S93	**S143**	**Y144**	**A166**	**S167**	***K377***	R243	**R271**	S272	**G296**	L300
mGlu3R	R64	*R68*	S100	S149	Y150	A172	S173	*K389*	R249	R277	S278	G302	Q306
mGlu4R	**K74**	***R78***	S110	**S157**	**G158**	**A180**	**S181**	***K405***	**R258**	**N286**	E287	**S313**	**K317**
mGlu6R	Q58	*R62*	S94	S146	A147	A169	S170	*K394*	R247	N275	E276	S302	K306
mGlu7R	N74	*R78*	S110	S157	G158	A180	S181	*K407*	Q258	N288	D289	S315	K319
mGlu8R	K71	*R75*	S107	A154	A155	A177	S178	*K401*	R255	N283	E284	S310	K314

[a] Residues that interact directly with the agonist distal function, through polar or van der Waals contact as detected by the WHATIF program[19] for the docking models, are bold, and conserved ones are in italic.

Table 3), binding of the distal acidic group is markedly different for each receptor subtype. This is in contrast with the highly conserved binding of the proximal functions. In fact, a set of several binding residues from this region (Table 3) is characteristic of each pharmacological group and is responsible for group selectivity. These residues can bind to specific chemical groups held by the ligands, but they also affect the disposition of the distal carboxylate relative to the ligand glycine moiety and protein backbone (Figure 1). Among these residues, Tyr74 and Ser186 from mGlu1R seem to be responsible for the restricted length of well-accepted agonists as illustated with 4-acidic phenylglycines turned into antagonists. On the other hand, in mGlu2 and mGlu4 subtypes, Ser143/Arg57 and Ser157/Lys74, respectively, would be responsible for the longer agonist tolerance. Indeed, Ser186 (mGlu1R) is much closer to the proximal region than Ser143/118 (mGlu2/4R). Also, Arg57 (mGlu2R) and Lys74 (mGlu4R) hold more flexible side chains than Tyr74 (mGlu1R) and can adapt to variable agonist lengths. These residues also have a major influence on the relative disposition of the distal carboxylate or its isostere. As seen in Figure 1, this group is more tucked into lobe I in the mGlu2/4R models than in the mGlu1R model. It allows wider agonists, such as LY354740, to bind at mGlu2R and not at mGlu1R. It also affects the position of possible bridging water molecules which can be displaced with larger agonists (e.g., quisqualate, (*S*)-3,5-DHPG, (*S*)-4-CPG, (*S*)-PPG, and (*S*)-DCPG). In our mGlu2R models, Arg57 and Ser143 appear as the only polar specific residues, while Lys74, Ser157, Arg258, Asn286, Ser313, and Lys317 constitute a highly basic and hydrophilic cluster around the distal function of mGlu4R. Thus, we explain why group III specific agonists ((*S*)-AP4 **12**, ACPT-I **13**, and (*S*)-PPG **15**) hold an additional distal acidic function which is well suited to this environment. Some specificity might also be connected to some hydrophobic residues close to the hinge region which are brought in contact when agonists are bound (Figure 7C).

Agonist Affinity and Potency. The recent crystallographic structures of the LBD of mGlu1R as a dimer have suggested a new receptor activation mechanism in which the relative orientation of the two binding domains would be critical.[4,8,20,26] At least one closed conformation of this domain would be required for activation. A recent theoretical model established how the conformation of the LBD controls the activity of the receptor.[27] An increase in the proportion of the closed state due to agonist binding would increase the proportion of active state receptors. Our results are in agreement with the proposed thermodynamic model.

At the mGlu1R binding site, glutamate γ-carboxylate is bound to Tyr74, Ser186 via a water molecule, Gly293 via a water molecule, Arg323 in addition to the conserved Lys409 and Arg78 according to the crystal structure.[20] (*S*)-3,5-DHPG **3** and quisqualate **2** fit optimally to these residues without bridging water molecules. In the diphenol ring, as well as in the dioxo-oxadiazolidine ring, the two hydroxyl or carbonyl groups are in such relative disposition that they allow simultaneous binding to Tyr74 and Ser186 from lobe I and to Gly293 and Arg323 from lobe II (Figure 2). Thus, a tight linkage of the two lobes is achieved, inducing a shift to the active form of the ATD. However, the weaker affinity of **3** may be due to a weaker cation$-\Pi$ interaction between the aromatic ring of **3** and the ammonium of Lys409 in place of an ionic interaction. At the mGlu2R binding site, hydrophobic effects between the ligand and lobe II seem to be major factors for the increased stability of the closed form of the ATD when bound with these agonists. In fact, glutamate and its analogues are brought into contact with a lipophilic surface from lobe II upon closing of the two lobes. This lipophilic environment results essentially from Tyr144 and Tyr216 aromatic rings and the methylene side chain of Arg271. The stronger potency of **6** compared to that of **4** or **5** can be explained by the combination of a restricted flexibility and a larger hydrophobic surface, while the additional potency of **11** might originate from additional hydrogen bonds via a water molecule (Figure 6). In the case of mGlu4R, the active form of the ATD is stabilized by an increased number of polar bonds (ionic or hydrogen bonds) between the agonist and the receptor.

In the present article, the dockings of several agonists which are more potent than glutamate are described. We note that favorable entropy and additional contacts can provide increased stability of the closed conformation which correlates with their higher affinity and potency. Moreover, we suggest that receptor activation occurs when the bilobate domain closes to a precise angle as is the case with the GluR2 ligand binding core.[50] Thus, ligands that fit into the cleft and lock this conformation are expected to be among the most potent agonists: quisqualate and LY354740 are of this type. Ligands with high affinity but which induce a different closing angle would be partial agonists or antagonists. This hypothesis has been validated while this paper was under revision.[23]

Interlobe Connections. It has been shown that the equilibrium between open and closed conformations takes place in the absence of ligand/agonist for both the periplasmic binding proteins[59] and mGlu1R ATD.[20] Indeed, several interlobe connections can be established

when the unliganded ATD closes.[20] The same clamps are found in the closed-liganded ATD. When a ligand prevents the closing motion of the ATD, these connections cannot occur, and the receptor activation is perturbed. Such a situation is met, for example, with **8**, the 6-fluoro analogue of LY354740,[12] or with several α-methylglutamate analogues[5,6] which are, in fact, competitive antagonists. Further description will be reported in a subsequent article. Here, we describe connections that are situated around the agonist in the closed conformation of the LBD. As we noted that the proximal functions of glutamate analogues are bound to conserved residues, we observed that interlobe connections in this region are also conserved (panels A and B of Figure 9). On the other hand, connections in the environment of the agonist distal function are more diverse (Figure 9C), as seen with ligand binding.

Conclusion

We have described the docking of 8 agonists at their respective mGluR binding sites. Common binding for the glycine moiety has been detected, while selective interactions are described for the distal functions. Several interlobe connections are established around the ligand and participate in the tight closing of the bilobate structure. Altogether, our results show that increased affinity and potency of better agonists compared to glutamate would be related to improved binding to the mGluR ATD closed form. Thus, the stabilization of this conformation would induce a shift of the receptor equilibrium to its active form.

Materials and Methods

Homology Models for mGlu2R and mGlu4R ATD Closed Forms. Both homology modeling models for mGlu2R and mGlu4R LBD closed forms were generated by the automated homology modeling tool MODELER 5.00 (InsightII, version 2000, Accelrys, San Diego, CA).[60] Models were generated by using the coordinates of the LBD domain of mGlu1R closed form bound with glutamate (1ewk:A) and based on a sequence alignment previously described.[19] To properly position the glutamate in our homology models, we used the HETATM_IO routine available in MODELER 5.00. The structural quality of the models was assessed according to MODELER's probability density function and Profiles-3D analysis (InsightII, version 2000).[61] The selected models were further used for docking.

Docking. Two or more of the most potent and/or selective mGluR agonists (Chart 1) were selected for each group: quisqualic acid **2**, (*S*)-3,5-dihydroxyphenylglycine **3** (3,5-DHPG), (+)-2-aminobicyclo[3.1.0]hexane-2,6-dicarboxylic acid **6** (LY354740), (2*S*,2′*S*,3′*R*)-2-(2′,3′-dicarbocarboxycyclopropyl)-glycine **5** (DCG-IV), (1*S*,3*R*,4*S*)-1-aminocyclopentane-1,3,4-tricarboxylic acid **13** (ACPT-I), and (*S*)-2-amino-4-phosphonobutyric acid **12** ((*S*)-AP4). They were docked into the active site of mGlu1R ATD (1ewk:A), mGlu2R ATD, and mGlu4R ATD (homology modeling models). The ligands were first manually positioned in their bioactive conformations[17,18] by superimposing their glycine moiety on the amino acid function of glutamate. The obtained protein−ligand complex was, therefore, submitted to energy minimization (steepest-descent convergence, 2 kcal mol^{-1} Å^{-1}; conjugate-gradient convergence, 0.1 kcal mol^{-1} Å^{-1}) while tethering the Cα trace. This was performed using the Discover 3.00 calculation engine with the CFF force field (InsightII, version 2000). The nonbond cutoff method and dielectric constant were set to cell-multipole and distance dependent ($\epsilon = 1R$), respectively. Discover 3.00 and the CFF force field were further used to perform 400 ps of molecular dynamics at 298 K. The Cα trace was tethered using a quadratic potential during the entire protocol (general protocol) except in the docking of quisqualate **2**, LY354740 **6**, and (*S*)-AP4 **12**, where it was gradually released from 100 to 0 kcal mol^{-1} Å^{-2}. The integration time step was set to 1 fs, and the calculations were performed at constant volume and temperature. Once the system was equilibrated, the coordinates of snapshots collected over a period of 20 ps were averaged and submitted again to energy minimization (steepest-descent convergence, 2 kcal mol^{-1} Å^{-1}; conjugate-gradient convergence, 0.01 kcal mol^{-1} Å^{-1}; Cα trace tethered). The same minimization protocol was used when water molecules were added.

Model Scoring. Scoring of the poses of the different agonists, with respect to the 3 subtypes of receptors, was performed using the LigandFit module implemented in Cerius2.[44] Conformations of both ligand and protein were obtained from the previously described simulation protocols.

The determination of the binding region was based on the shape of the docked ligands. Several scoring functions were used, such as Ligscore,[44] PLP1,[45]and PMF.[46] Two versions of PMF were used; they are indicated as PMF_H and PMF and include or do not include hydrogen atoms, respectively. Ligscore was used in conjunction with the CFF force field (Accelrys).

Acknowledgment. This work was supported by grants from the CNRS, the "Action incitative Physique et Chimie du Vivant" (PCV00-134), the "Action Molécules et Cibles Thérapeutiques" from CNRS/INSERM, and by RETINA France. The authors thank Parke-Davis Pharmaceutical Research (Ann Arbor MI) for allowing a Fullbright scholarship to A.-S.B. and Nicolas Triballeau for constructive discussions.

References

(1) Parthasarathy, H. S., Ed. Neurological disorders. *Nature* **1999**, *399* (Suppl.), A1−A47.
(2) Conn, P. J.; Pin, J.-P. Pharmacology and functions of metabotropic glutamate receptors. *Annu. Rev. Pharmacol. Toxicol.* **1997**, *37*, 205−237.
(3) Schoepp, D. D. Unveiling the functions of presynaptic metabotropic glutamate receptors in the central nervous system. *J. Pharmacol. Exp. Ther.* **2001**, *299*, 12−20.
(4) Pin, J. P.; Bockaert, J. Type III Family of GPCRs − Metabotropic glutamate receptors. In *Structure and function of GPCRs in the Nervous System*; Pangalos, M. N., Davies, C. H., Eds.; Oxford University Press: Oxford, U.K., in press, 2002.
(5) Pin, J.-P.; De Colle, C.; Bessis, A.-S.; Acher, F. New perspective in the development of selective metabotropic glutamate receptor ligands. *Eur. J. Pharmacol.* **1999**, *375*, 277−294.
(6) Schoepp, D. D.; Jane, D. E.; Monn, J. A. Pharmacological agents acting at subtypes of metabotropic glutamate receptors. *Neuropharmacology* **1999**, *38*, 1431−1476.
(7) Bräuner-Osborne, H.; Egebjerg, J.; Nielsen, B.; Madsen, U.; Krogsgaard-Larsen, P. Ligands for glutamate receptors: design and therapeutic prospects. *J. Med. Chem.* **2000**, *43*, 2609−2645.
(8) Pin, J.-P.; Acher, F. The metabotropic glutamate receptors: structure, activation mechanism and pharmacology. *Curr. Drug Targets: CNS Neurol. Disord.*, in press, 2002.
(9) Brabet, I.; Parmentier, M.-L.; De Colle, C.; Bockaert, J.; Acher, F.; Pin, J.-P. Comparative effect of L-CCG-I, DCG-IV and γ-carboxy-L-glutamate on all cloned metabotropic glutamate receptor subtypes. *Neuropharmacology* **1998**, *37*, 1043−1051.
(10) Monn, J. A.; Valli, M. J.; Massey, S. M.; Wright, R. A.; Salhoff, C. R.; Johnson, B. G.; Howe, T.; Alt, C. A.; Rhodes, G. A.; Robey, R. L.; Griffey, K. R.; Tizzano, J. P.; Kallman, M. J.; Helton, D. R.; Schoepp, D. D. Design, synthesis, and pharmacological characterization of (+)-2-aminobicyclo[3.1.0]hexane-2,6-dicarboxylic acid (LY354740): a potent, selective, and orally active group 2 metabotropic glutamate receptor agonist possessing anticonvulsant and anxiolytic properties. *J. Med. Chem.* **1997**, *40*, 528−537.
(11) Monn, J. A.; Valli, M. J.; Massey, S. M.; Hansen, M. M.; Kress, T. J.; Wepsiec, J. P.; Harkness, A. R.; Grutsch, J. L.; Wright, R.

A.; Jonhson, B. G.; Andis, S. L.; Kingston, A.; Tomlinson, R.; Lewis, R.; Griffey, K. R.; Tizzano, J. P.; Schoepp, D. D. Synthesis, pharmacological characterization, and molecular modeling of hetero bicyclic amino acids related to (+)-2-aminobicyclo[3.1.0]-hexane-2,6-dicarboxylic acid (LY354740): identification of two new potent, selective, systemically active agonists for group II metabotropic glutamate receptors. *J. Med. Chem.* **1999**, *42*, 1027−1040.

(12) Nakazato, A.; Kumagai, T.; Sakagami, K.; Yoshikawa, R.; Suzuki, Y.; Chaki, S.; Ito, H.; Taguchi, T.; Nakanishi, S.; Okuyama, S. Synthesis, SARs, and Pharmacological Characterization of 2-Amino-3 or 6-fluorobicyclo[3.1.0]hexane-2,6-dicarboxylic Acid Derivatives as Potent, Selective, and Orally Active Group II Metabotropic Glutamate Receptor Agonists. *J. Med. Chem.* **2000**, *43*, 4893−4909.

(13) Acher, F.; Tellier, F.; Brabet, I.; Fagni, L.; Azerad, R.; Pin, J.-P. Synthesis and pharmacological characterization of aminocyclopentane tricarboxylic acids (ACPT): new tools to discriminate between metabotropic glutamate receptor subtypes. *J. Med. Chem.* **1997**, *40*, 3119−3129.

(14) De Colle, C.; Bessis, A.-S.; Bockaert, J.; Acher, F.; Pin, J.-P. Pharmacological characterization of the rat metabotropic glutamate receptor type 8a revealed strong similarities and slight differences with the type 4a receptor. *Eur. J. Pharmacol.* **2000**, *394*, 17−26.

(15) Gasparini, F.; Inderbitzin, W.; Francotte, E.; Lecis, G.; Richert, P.; Dragic, Z.; Kuhn, R.; Flor, P. J. (+)-Phosphonophenylglycine (PPG): a new group III selective metabotropic glutamate receptor agonist. *Bioorg. Med. Chem. Lett.* **2000**, *10*, 1241−1244.

(16) Thomas, N. K.; Wright, R. A.; Howson, P. A.; Kingston, A. E.; Schoepp, D. D.; Jane, D. E. (*S*)-3,4-DCPG, a potent and selective mGlu8a receptor agonist, activates metabotropic glutamate receptors on primary afferent terminals in the neonatal rat spinal cord. *Neuropharmacology* **2001**, *40*, 311−318.

(17) Jullian, N.; Brabet, I.; Pin, J.-P.; Acher, F. Agonist selectivity of mGluR1 and mGluR2 metabotropic receptors: a different environment but similar recognition of an extended glutamate conformation. *J. Med. Chem.* **1999**, *42*, 1546−1555.

(18) Bessis, A.-S.; Jullian, N.; Coudert, E.; Pin, J.-P.; Acher, F. Extended glutamate activates metabotropic receptor types 1, 2 and 4: selective features at mGluR4 binding site. *Neuropharmacology* **1999**, *38*, 1543−1551.

(19) Bessis, A.-S.; Bertrand, H.-O.; Galvez, T.; De Colle, C.; Pin, J.-P.; Acher, F. Three-dimensional model of the extracellular domain of the type 4a metabotropic glutamate receptor: new insights into the activation process. *Protein Sci.* **2000**, *9*, 2200−2209.

(20) Kunishima, N.; Shimada, Y.; Tsuji, Y.; Sato, T.; Yamamoto, M.; Kumasaka, T.; Nakanishi, S.; Jingami, H.; Morikawa, K. Structural basis of glutamate recognition by a dimeric metabotropic glutamate receptor. *Nature* **2000**, *407*, 971−977.

(21) O'Hara, P. J.; Sheppard, P. O.; Thogersen, H.; Venezia, D.; Haldeman, B. A.; McGrane, V.; Houamed, K. H.; Thomsen, C.; Gilbert, T. L.; Mulvihill, E. R. The ligand-binding domain in metabotropic glutamate receptors is related to bacterial periplasmic binding proteins. *Neuron* **1993**, *11*, 41−52.

(22) Hampson, D. R.; Huang, X.-P.; Pekhletski, R.; Peltekova, V.; Hornby, G.; Thomsen, C.; Thøgersen, H. Probing the ligand-binding domain of the mGluR4 subtype of metabotropic glutamate receptor. *J. Biol. Chem.* **1999**, *274*, 33488−33495.

(23) Tsuchiya, D.; Kunishima, N.; Kamiya, N.; Jingami, H.; Morikawa, K. Structural views of the ligand-binding cores of a metabotropic glutamate receptor complexed with an antagonist and both glutamate and Gd3+. *Proc. Natl. Acad. Sci. U.S.A.* **2002**, *99*, 2660−2665.

(24) Gerstein, M.; Lesk, A. M.; Chothia, C. Structural mechanisms for domain movements in proteins. *Biochemistry* **1994**, *33*, 6739−6749.

(25) Romano, C.; Yang, N. L.; O'Malley, K. L. Metabotropic glutamate receptor is a disulfide-linked dimer. *J. Biol. Chem.* **1996**, *271*, 28612−28616.

(26) Gasparini, F.; Kuhn, R.; Pin, J.-P. Allosteric modulators of group I metabotropic glutamate receptors: novel subtype-selective ligands and therapeutic perspectives. *Curr. Opin. Pharmacol.* **2002**, *2*, 43−49.

(27) Parmentier, M.-L.; Prézeau, L.; Bockaert, J.; Pin, J.-P. A model for the functioning of family 3 GPCRs. *Trends Pharmacol. Sci.*, in press, 2002.

(28) Eriksen, L.; Thomsen, C. [^{3}H]-L-2-Amino-4-phosphonobutyrate labels a metabotropic glutamate receptor, mGluR4a. *Br. J. Pharmacol.* **1995**, *116*, 3279−3287.

(29) Cartmell, J.; Adam, G.; Chaboz, S.; Henningsen, R.; Kemp, J. A.; Klingelschmidt, A.; Metzler, V.; Monsma, F.; Schaffhauser, H.; Wichmann, J.; Mutel, V. Characterization of [^{3}H]-(2*S*,2′*R*,3′*R*)-2-(2′,3′-dicarboxycyclopropyl)glycine ([^{3}H]-DCG IV) binding to metabotropic mGlu$_2$ receptor-transfected cell membranes. *Br. J. Pharmacol.* **1998**, *123*, 497−504.

(30) Johnson, B. G.; Wright, R. A.; Arnold, M. B.; Wheeler, W. J.; Ornstein, P. L.; Schoepp, D. D. [^{3}H]-LY341495 as a novel antagonist radioligand for group II metabotropic glutamate (mGlu) receptors: characterization of binding to membranes of mGlu receptor subtype expressing cells. *Neuropharmacology* **1999**, *38*, 1519−1529.

(31) Wright, R. A.; Arnold, M. B.; Wheeler, W. J.; Ornstein, P. L.; Schoepp, D. D. Binding of [^{3}H](2*S*,1′*S*,2′*S*)-2-(9-xanthylmethyl)-2-(2′-carboxycyclopropyl) glycine ([^{3}H]LY341495) to cell membranes expressing recombinant human group III metabotropic glutamate receptor subtypes. *Naunyn-Schmiedeberg's Arch. Pharmacol.* **2000**, *362*, 546−554.

(32) Mutel, V.; Ellis, G. J.; Adam, G.; Chaboz, S.; Nilly, A.; Messer, J.; Bleuel, Z.; Metzler, V.; Malherbe, P.; Schlaeger, E. J.; Roughley, B. S.; Faull, R. L.; Richards, J. G. Characterization of [^{3}H]Quisqualate binding to recombinant rat metabotropic glutamate 1a and 5a receptors and to rat and human brain sections. *J. Neurochem.* **2000**, *75*, 2590−2601.

(33) Schweitzer, C.; Kratzeisen, C.; Adam, G.; Lundstrom, K.; Malherbe, P.; Ohresser, S.; Stadler, H.; Wichmann, J.; Woltering, T.; Mutel, V. Characterization of [^{3}H]-LY354740 binding to rat mGlu2 and mGlu3 receptors expressed in CHO cells using semliki forest virus vectors. *Neuropharmacology* **2000**, *39*, 1700−1706.

(34) Naples, M. A.; Hampson, D. R. Pharmacological profiles of the metabotropic glutamate receptor ligands [^{3}H]L-AP4 and [^{3}H]-CPPG. *Neuropharmacology* **2001**, *40*, 170−177.

(35) Kellogg, G. E.; Burnett, J. C.; Abraham, D. J. Very empirical treatment of solvation and entropy: a force field derived from log Po/w. *J. Comput.-Aided Mol. Des.* **2001**, *15*, 381−393.

(36) Kollman, P. A.; Massova, I.; Reyes, C.; Kuhn, B.; Huo, S.; Chong, L.; Lee, M.; Lee, T.; Duan, Y.; Wang, W.; Donini, O.; Cieplak, P.; Srinivasan, J.; Case, D. A.; Cheatham, T. E. r. Calculating structures and free energies of complex molecules: combining molecular mechanics and continuum models. *Acc. Chem. Res.* **2000**, *33*, 889−897.

(37) Gallivan, J. P.; Dougherty, D. A. Cation-Π interactions in structural biology. *Proc. Natl. Acad. Sci. U.S.A.* **1999**, *96*, 9459−9464.

(38) Nishio, M.; Umezawa, Y.; Hirota, M.; Takeuchi, Y. The CH/Π interaction: significance in molecular recognition. *Tetrahedron* **1995**, *51*, 8665−8701.

(39) D'Aquino, J. A.; Freire, E.; Amzel, L. M. Binding of small organic molecules to macromolecular targets: evaluation of conformational entropy changes. *Proteins* **2000** (Suppl. 4), 93−107.

(40) Klebe, G.; Gradler, U.; Gruneberg, S.; Kramer, O.; Gohkle, H. Virtual screening for bioactive molecules: understanding receptor ligand interactions as prerequisite for virtual screening. In *Methods and Principles in Medicinal Chemistry*; Mannhold, R., Kubinyi, H., Timmerman, H., Eds.; Wiley-VCH: Weinheim, Germany, 2000; Vol. 10, pp 207−227.

(41) Matsushima, A.; Fujita, T.; Nose, T.; Shimohigashi, Y. Edge-to-face CH/Π interaction between ligand Phe-Phenyl and receptor aromatic group in the thrombin receptor activation. *J. Biochem.* **2000**, *128*, 225−232.

(42) Rablen, P. R.; Lockman, J. W.; Jorgensen, W. L. Ab initio study of hydrogen-bonded complexes of small organic molecules with water. *J. Phys. Chem. A* **1998**, *102*, 3782−3797.

(43) Bessis, A.-S.; Bolte, J.; Pin, J.-P.; Acher, F. New probes of the agonist binding site of metabotropic glutamate receptors. *Bioorg. Med. Chem. Lett.* **2001**, *11*, 1569−1572.

(44) *Cerius2*, version 4.6; Accelrys: San Diego, CA, 2000.

(45) Gehlhaar, D. K.; Verkhivker, G. M.; Rejto, P. A.; Sherman, C. J.; Fogel, D. B.; Fogel, L. J.; Freer, S. T. Molecular Recognition of the Inhibitor AG-1343 by HIV-1 Protease: Conformationally Flexible Docking by Evolutionary Programming. *Chem. Biol.* **1995**, *2*, 317−324.

(46) Muegge, I.; Martin, Y. C. A general and fast scoring function for protein−ligand interactions: a simplified potential approach. *J. Med. Chem.* **1999**, *42*, 791−804.

(47) Gohlke, H.; Klebe, G. Statistical potentials and scoring functions applied to protein−ligand binding. *Curr. Opin. Struct. Biol.* **2001**, *11*, 231−235.

(48) Ha, S.; Andreani, R.; Robbins, A.; Muegge, I. Evaluation of docking/scoring approaches: a comparative study based on MMP3 inhibitors. *J. Comput.-Aided Mol. Des.* **2000**, *14*, 435−448.

(49) Terp, G. E.; Johansen, B. N.; Christensen, I. T.; Jorgensen, F. S. A new concept for multidimensional selection of ligand conformations (MultiSelect) and multidimensional scoring (MultiScore) of protein−ligand binding affinities. *J. Med. Chem.* **2001**, *44*, 2333−2343.

(50) Armstrong, N.; Gouaux, E. Mechanisms for activation and antagonism of an AMPA-sensitive glutamate receptor: crystal

structures of the GluR2 ligand binding core. *Neuron* **2000**, *28*, 165−181.
(51) Sack, J. S.; Saper, M. A.; Quiocho, F. A. Periplasmic binding protein structure and function. Refined X-ray structures of the leucine/isoleucine/valine-binding protein and its complex with leucine. *J. Mol. Biol.* **1989**, *206*, 171−191.
(52) Sack, J. S.; Trakhanov, S. D.; Tsigannik, I. H.; Quiocho, F. A. Structure of the L-leucine-binding protein refined at 2.4 Å resolution and comparaison with the Leu/Ile/Val-binding protein structure. *J. Mol. Biol.* **1989**, *206*, 193−207.
(53) Parmentier, M.-L.; Galvez, T.; Acher, F.; Peyre, B.; Pellicciari, R.; Grau, Y.; Bockaert, J.; Pin, J.-P. Conservation of the ligand recognition site of metabotropic glutamate receptors during evolution. *Neuropharmacology* **2000**, *39*, 1119−1131.
(54) Conigrave, A. D.; Quinn, S. J.; Brown, E. M. L-Amino acid sensing by the extracellular Ca^{2+}-sensing receptor. *Proc. Natl. Acad. Sci. U.S.A.* **2000**, *97*, 4814−4819.
(55) Speca, D. J.; Lin, D. M.; Sorensen, P. W.; Isacoff, E.; Ngai, J.; Dittman, A. H. Functional identification of a goldfish odorant receptor. *Neuron* **1999**, *23*, 487−498.
(56) Raymer, M. L.; Sanschagrin, P. C.; Punch, W. F.; Venkataraman, S.; Goodman, E. D.; Kuhn, L. A. Predicting conserved water-mediated and polar ligand interactions in proteins using a K-nearest-neighbors genetic algorithm. *J. Mol. Biol.* **1997**, *265*, 445−464.
(57) Rarey, M.; Kramer, B.; Lengauer, T. The particle concept: placing discrete water molecules during protein−ligand docking predictions. *Proteins* **1999**, *34*, 17−28.
(58) Finley, J. B.; Atigadda, V. R.; Duarte, F.; Zhao, J. J.; Wayne, J.; Brouillette, W. J.; Air, G. M.; Luo, M. Novel aromatic inhibitors of influenza virus neuraminidase make selective interactions with conserved residues and water molecules in the active site. *J. Mol. Biol.* **1999**, *293*, 1107−1119.
(59) Quiocho, F. A.; Ledvina, P. S. Atomic structure and specificity of bacterial periplasmic receptors for active transport and chemotaxis: variation of common themes. *Mol. Microbiol.* **1996**, *20*, 17−25.
(60) Sali, A.; Blundell, T. L. Definition of general topological equivalence in protein structures: A procedure involving comparison of properties and relationships through simulated annealing and dynamic programming. *J. Mol. Biol.* **1990**, *212*, 403−428.
(61) Luthy, R.; Bowie, J. U.; Eisenberg, D. Assessment of protein models with three-dimensional profiles. *Nature* **1992**, *356*, 83−85.
(62) Han, G.; Hampson, D. R. Ligand binding to the amino-terminal domain of the mGluR4 subtype of metabotropic glutamate receptor. *J. Biol. Chem.* **1999**, *274*, 10008−10013.

JM010323L